ISSN 1070-3632, Russian Journal of General Chemistry, 2015, Vol. 85, No. 9, pp. 2149–2162. © Pleiades Publishing, Ltd., 2015.

Synthesis and Spectral, Antimicrobial, Anion Sensing, and DNA Binding Properties of Schiff Base Podands and Their Metal Complexes[1]

M. Yıldız[a, b], E. Tan[a], N. Demir[c], N. Yıldırım[d], H. Ünver[e], A. Kiraz[f], and B. Mestav[g]

[a] *Department of Chemistry, Faculty of Arts and Sciences, Çanakkale Onsekiz Mart University, Çanakkale, 17100 Turkey*
e-mail: myildiz@comu.edu.tr

[b] *Nanoscience and Technology Research and Application Center (NANORAC), Çanakkale Onsekiz Mart University, Çanakkale, Turkey*

[c] *Department of Biology, Faculty of Arts and Sciences, Çanakkale Onsekiz Mart University, Çanakkale, 17100 Turkey*

[d] *Health Services Vocational School, Çanakkale Onsekiz Mart University, 17100 Çanakkale, Turkey*

[e] *Department of Physics, Faculty of Sciences, Ankara University, TR-06100, Ankara, Turkey*

[f] *Ataturk Faculty of Education, Near East University, Nicosia, Mersin 10 Turkey*

[g] *Department of Statistics, Faculty of Arts and Sciences, Çanakkale Onsekiz Mart University, Çanakkale, 17100 Turkey*

Received May 5, 2015

Abstract—Schiff base podands have been synthesized by reaction of triethylene glycol bis(4-aminophenyl) ether with salicylaldehyde, 5-substituted salicylaldehydes, and 2-hydroxy-1-naphthaldehyde. Manganese(II), iron(II), cobalt(II), nickel(II), and copper(II) complexes have been prepared from the salicylaldehyde-based podand via reaction with $MCl_2 \cdot nH_2O$. The structures of the ligands and complexes have been studied by elemental analysis, FT-IR and UV-visible spectroscopy, ^1H and ^{13}C NMR, and thermogravimetric analysis. The UV-visible spectral and TG data suggest tetrahedral geometry of the metal complexes. The antimicrobial activities of the ligands and metal complexes have been evaluated as minimum inhibitory concentrations with respect to bacteria and yeast cultures. The interaction of the Schiff base podands with calf thymus DNA has been investigated by UV-visible spectroscopy, and intercalative binding to DNA has been found. The anion recognition ability of all Schiff base podands has been examined by UV-visible spectroscopy. A visually detectable color change has been observed upon addition of fluoride, cyanide, hydroxide, and acetate ions due to formation of 1 : 1 H-complexes and/or deprotonation of the receptor. No significant color change has been observed upon addition of other anions such as dihydrogen phosphate, bromide, iodide, thiocyanate, perchlorate, and hydrogen sulfate.

Keywords: Schiff base, tautomerism, metal complexes, podand, minimum inhibitory concentration, calf thymus-DNA, colorimetric sensors

DOI: 10.1134/S1070363215090200

Schiff bases have been reported to exhibit biological activity such as antibacterial, antifungal, anti-inflammatory, analgesic, anticonvulsant, antitubercular, anticancer, antioxidant, and anthelmintic [1–19]. Metal complexes derived from Schiff bases have applications in the area of materials to biological sciences. They have been widely studied because they have anticancer and herbicidal applications [20, 21]. Schiff base complexes show greater biological activity than free ligands [3, 22]. They serve as models for biologically important species [23]. Some Schiff base cobalt complexes are potent antiviral agents [24]. Schiff base copper(II) complexes can bind to DNA and induce apoptosis and show cytotoxicity [25–29]. They can cause free radical damage to DNA of cancer cells [30–33]. Synthesis of sensors for the recognition and sensing of anions is one of the most importing areas of different sciences [34–38]. Over the past few years,

[1] The text was submitted by the authors in English.

Scheme 1.

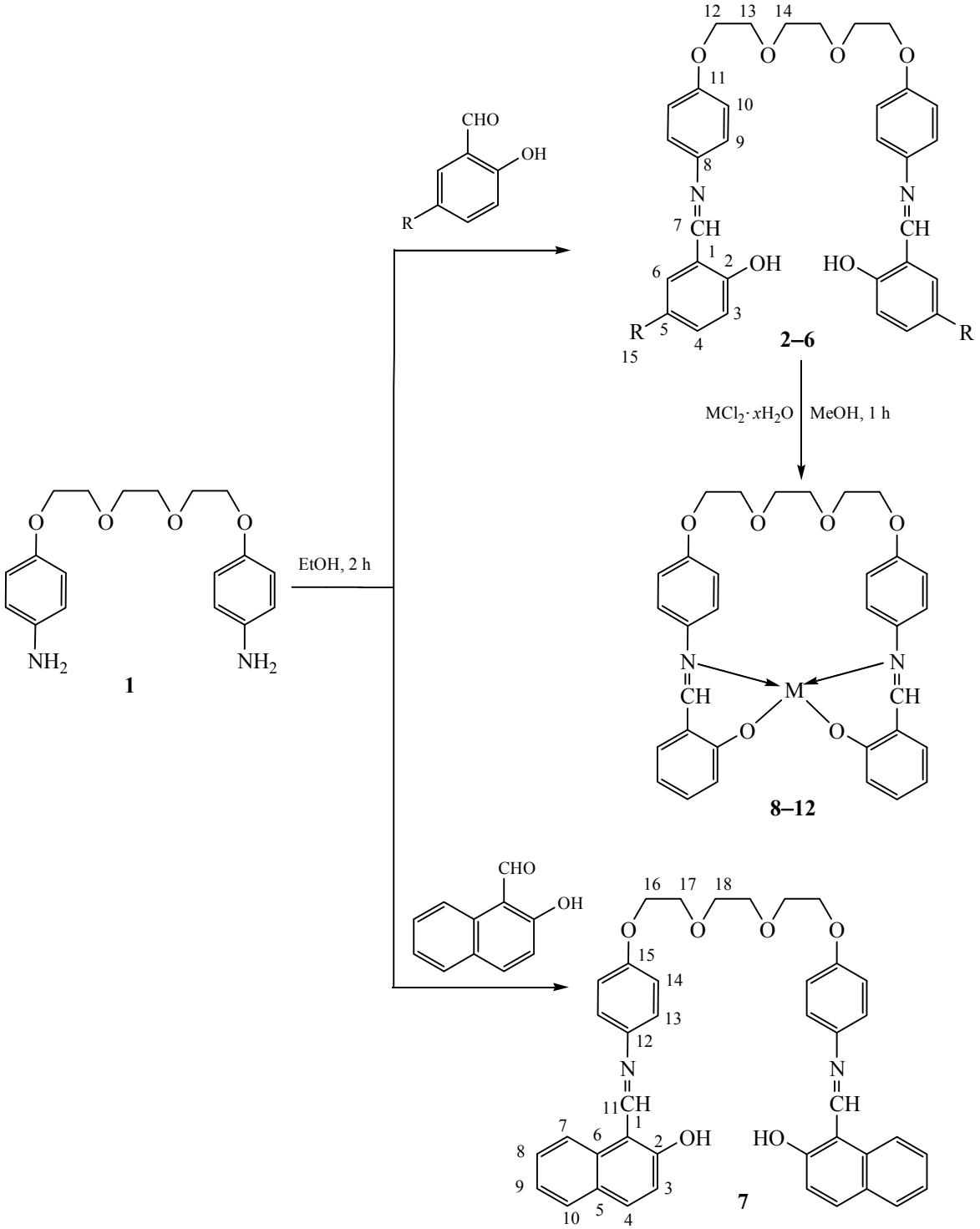

2, R = H; **3**, R = Cl; **4**, R = Br; **5**, R = HO; **6**, R = MeO; **8**, M = Mn; **9**, M = Fe; **10**, M = Co; **11**, M = Ni; **12**, M = Cu.

much effort has been made to develop fluorescent chemosensors for the detection of various anions, taking into account high sensitivity of fluorometric detection. However, UV-Vis absorption spectroscopy and colorimetric naked-eye detection techniques have gained comparatively greater attention than other techniques due to their simplicity, high sensitivity, and cost effectiveness [39–42]. Tautomerism of Schiff

Table 1. Yields, melting points, and elemental analyses of Schiff base podands **2–7** and complexes **8–12**

Compound no.	Yield, %	mp, °C	Color	Calculated, %			Formula	*M*	Found, %		
				C	H	N			C	H	N
2	88	115	Yellow	71.11	5.92	5.18	$C_{32}H_{32}N_2O_6$	540	71.13	5.97	5.18
3	78	156	Yellowish	63.05	4.92	4.59	$C_{32}H_{30}Cl_2N_2O_6$	609	63.11	4.96	4.60
4	80	163	Yellowish	55.01	4.29	4.01	$C_{32}H_{30}Br_2N_2O_6$	698	55.18	4.33	4.01
5	82	153	Brown	65.08	5.76	4.74	$C_{32}H_{32}N_2O_8 \cdot H_2O$	590	65.07	5.80	4.74
6	70	134	Yellowish	68.00	6.00	4.66	$C_{34}H_{36}N_2O_8$	600	68.16	6.04	4.65
7	84	182	Yellow	72.94	5.77	4.25	$C_{40}H_{36}N_2O_8 \cdot H_2O$	658	72.93	5.82	4.25
8	82	329	Brownish				$C_{32}H_{30}N_2O_6Mn$	593			
9	88	340	Brown				$C_{32}H_{30}N_2O_6Fe$	594			
10	78	384	Brown				$C_{32}H_{30}N_2O_6Co$	597			
11	80	372	Brown				$C_{32}H_{30}N_2O_6Ni$	597			
12	88	387	Black				$C_{32}H_{30}N_2O_6Cu$	602			

bases containing a hydroxy group in the *ortho* position with respect to the imino group both in solution and in solid state has been studied using spectroscopy and X-ray crystallography techniques [3–8, 43–48]. Such Schiff bases attract interest mainly due to the existence of either O–H···N or O···H–N hydrogen bond and enol imine–amino ketone tautomerism. In some cases the OH hydrogen atom is completely transferred to the imino nitrogen; i.e., the enol imine–ketone amine equilibrium is displaced toward the latter. Schiff bases derived from 2-hydroxy-1-naphthaldehyde and aromatic amines exist mainly as ketone amine tautomers, whereas no ketone amine tautomer is observed in solution and solid state for Schiff bases derived from salicylaldehyde and aromatic amines.

Although a large number of Schiff base ligands obtained from aromatic and aliphatic amine have been reported, reactions of acyclic amino podands with substituted 2-hydroxy-1-benzaldehydes and 2-hydroxy-1-naphthaldehyde to produce new polyether Schiff base ligands have been described in a few publications [43, 49, 50]. In this work, some new acyclic polyether Schiff base ligands and their complexes with transition metals have been synthesized and tested for anti-microbial activity and DNA binding and anion sensing properties.

The new Schiff base podands **2–7** were synthesized by condensation of triethylene glycol bis(4-amino-phenyl) ether (**1**) with salicylaldehyde, its 5-substituted derivatives, and 2-hydroxy-1-naphthaldehyde (Scheme 1, Table 1). By reacting compound **2** with transition metal salts $MCl_2 \cdot x\ H_2O$ in methanol we obtained the corresponding metal complexes **8–12** (Scheme 1). The structure of the synthesized Schiff bases and complexes was determined by elemental analysis, FT-IR, UV-Vis, ^1H and ^{13}C NMR, and TG techniques.

Spectral data. The IR spectra of **2–12** (Table 2) displayed absorption bands at 1615–1625 [ν(C=N)], 3150–3041 [ν(C–H_{arom})], 2939–2866 [ν(C–H_{aliph})], 1603–1505 (C=C_{arom}), 1290–1106 [ν(C–O–C), ether], and 1392–1312 cm^{-1} [ν(C–O)]. The stretching frequency observed at 2882–2866 cm^{-1} in the spectra of **2–7** indicated the presence of O–H···N intramolecular hydrogen bond [43, 44]. The C=N stretching band is partly accountable for the existence of iminoenol tautomer. The compound with strong band at 1392–1312 cm^{-1} possesses the highest percentage of enol imine tautomer due to stabilization of the phenolic C–O bond [51]. The IR spectra of metal complexes **8–12** exhibited characteristic changes in the functional group frequencies compared with the free ligand (Fig. 1). The C=N stretching vibration band shifted to lower frequencies in going from ligand **2** to its Mn, Fe, Co, and Cu complexes, but it remained unchanged for the Ni complex.

The ^1H NMR spectra of **2–7** in DMSO-d_6 are given in Table 3. The ^1H NMR data for compounds **2–6** show that the tautomeric equilibrium is displaced

Table 2. IR spectra (ν, cm^{-1}) of compounds **2**–**12**

Compound no.	O–H (H_2O)	O–H	C–H_{arom}	C–H_{aliph}	C=N	C=C	C–O	C–O–C
2		3434 m	3041 m	2939 s, 2903 s, 2882 s	1621 s	1599 s	1363 m	1284 s, 1252 s, 1106 s
3		3433 br	3075 w	2927 s, 2870 s	1618 s	1598 s	1350 m	1275 s, 1252 s, 1181 s
4		3485 br	3150 m	2927 s, 2866 s	1615 s	1505 s	1385 m	1274 s, 1253 s, 1180 s
5		3390 br	3040 w	2905 m, 2880 m, 2793 m	1621 s	1603 s	1354 m, 1312 m	1290 s, 1253 s, 1131 s
6		3434 br	3059 w	2926 s, 2885 s	1625 s	1572 s	1397 s	1289 s, 1252 s, 1145 s
7		3434 br	3044 m	2926 s, 2878 s	1625 s	1508 s	1327 s	1250 s, 1176 s, 1129 s
8	3400 br	–	–	2928 m, 2875 m	1618 s	1508 s	1360 w	1282 s, 1252 s, 1145 s
9	3434 br	–	–	2924 s, 2880 s	1618 s	1508 s	1337 w	1284 s, 1252 s, 1132 s
10	3431 br	–	3071 m	2922 s, 2878 s	1610 s	1580 s	1385 m	1248 s, 1181 s, 1148 s
11	3400 br	–	–	2940 m, 2882 m	1621 s	1509 s	1360 w	1252 s, 1144 s, 1089 s
12	3434 br	–	3106 m	2924 s, 2851 s	1613 s	1506 s	1395 m	1253 s, 1120 s, 1087s

toward enol imine, while compound **7** prefers the ketone amine form in the same solvent. Protons of the ArOC$\underline{H_2}$C$\underline{H_2}$ group appeared as triplets, and OCH_2 proton signals were singlets. The OH and CH=N protons in **2**–**6** resonated as singlets, and those in **7** gave rise to a singlet and doublet, respectively. The ^{13}C NMR spectra of **2**–**7** (Table 4) displayed 14, 15, and 18 signals, respectively.

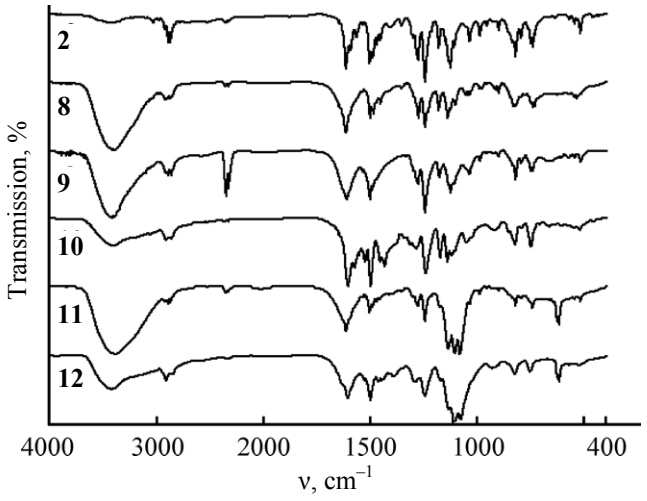

Fig. 1. FT-IR spectra of complexes **8**–**12**.

The UV-Vis spectra of **2**–**7** were studied in DMSO. It is known that Schiff bases with a hydroxy group in the *ortho* position with respect to the imino group in polar and nonpolar solvents in both acidic and basic media show absorption at λ values higher than 400 nm, which belongs to the ketone amine tautomer [43, 44]. An absorption band at λ > 400 nm was observed in DMSO for compound **7** but not for **2**–**6**. Thus, enol imine tautomer predominates in DMSO for **2**–**6**, while ketone amine predominates for **7** (55%). The UV-Vis spectra of **2**–**7** are shown in Fig. 2. The ligands displayed two broad bands at λ = 273 nm and 351 nm, which were assigned to π–π* and *n*–π* transitions of the C=C and C=N bonds. The position of these bands changes as a result of complexation (Fig. 3). The complexes did not show any *d*–*d* transition but displayed a charge transfer band at λ = 258–393 nm.

Table 3. ^{1}H NMR spectra (δ, ppm) of Schiff base podands **2**–**7** in DMSO-d_6

Compound no.	OH (2H)	N=CH (2H)	H_{arom}	$ArOCH_2$ (4H) (^3J, Hz)	$ArOCH_2CH_2$ (4H) (^3J, Hz)	OCH_2CH_2O (4H)
2	13.20 s	8.33 s	7.51–6.83 m (16H)	4.04 t (4.5)	3.68 t (4.5)	3.55 s
3	15.25 s	8.88 s	7.66–6.93 m (14H)	4.10 t (4.5)	3.75 t (4.5)	3.61 s
4	13.76 s	8.98 s	7.85–6.85 m (14H)	4.08 t (4.6)	3.72 t (4.6)	3.58 s
5	12.46 s, 9.07 s	8.79 s	7.37–6.74 m (16H)	4.10 t (4.5)	3.74 t (4.2)	3.61 s
6[a]	11.81 s	8.80 s	747–6.45 m (14H)	4.09 t (4.7)	3.74 t (4.5)	3.61 s
7	16.06 s	9.63 d (^3J = 3.1 Hz)	8.39–6.39 m (14H)	4.06 t (4.5)	3.83 t (4.5)	3.63 s

[a] 3.35 s (6H, OMe).

Table 4. ^{13}C NMR spectra (δ_C, ppm) of Schiff base podands **2**–**7** in DMSO-d_6 (for atom numbering, see Scheme 1)

Comp. no.	C^1	C^2	C^3	C^4	C^5	C^6	C^7	C^8	C^9	C^{10}	C^{11}	C^{12}	C^{13}	C^{14}	C^{15}	C^{16}	C^{17}	C^{18}
2	119.4	160.6	116.9	133.2	119.8	132.7	161.7	141.1	123.1	115.6	158.1	70.40	69.38	67.85				
3	121.2	159.3	121.1	132.6	123.2	131.3	160.1	140.9	122.8	115.7	158.4	70.40	69.35	67.86				
4	121.9	159.7	119.4	135.4	115.7	134.3	160.1	140.8	123.2	110.2	158.4	70.39	69.36	67.85				
5	122.9	153.4	119.8	120.9	150.0	117.5	161.4	141.5	123.1	115.6	158.1	70.37	69.38	67.82				
6	113.5	157.7	101.2	163.3	107.0	134.2	161.0	139.5	122.7	115.6	141.1	70.39	69.39	67.81	55.87			
7	115.8	160.4	121.0	136.5	133.4	152.3	123.7	128.4	122.4	129.4	169.5	155.0	122.2	120.8	157.8	70.41	69.39	67.90

Thermogravimetric analysis. Thermal studies (DTA-TGA) of the complexes were performed in the temperature range from 20–1200°C at a heating rate of 10 deg/min in air (Fig. 4). Manganese complex **8** decomposed in three steps. The first step (46–220°C) resulted in a weight loss of 8.7%, which corresponds to elimination of three water molecules. The second step (225–525°C) involves elimination of the $OC_2H_4O{\cdot}C_2H_4OC_2H_4O$ fragment (weight loss 31.3%). In the third step (550–950°C), two aniline and aldehyde fragments were lost (weight loss 18.5%), and a plateau was observed above 950°C due to formation of stable

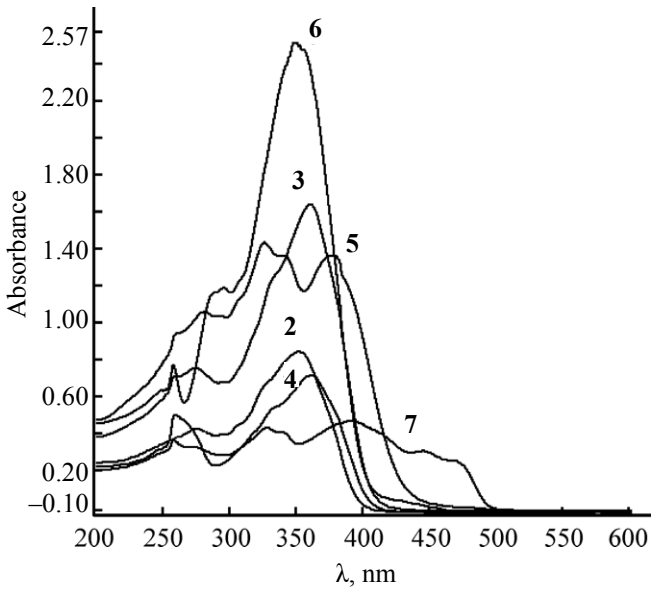

Fig. 2. UV-Vis spectra of compounds **2**–**7** in DMSO.

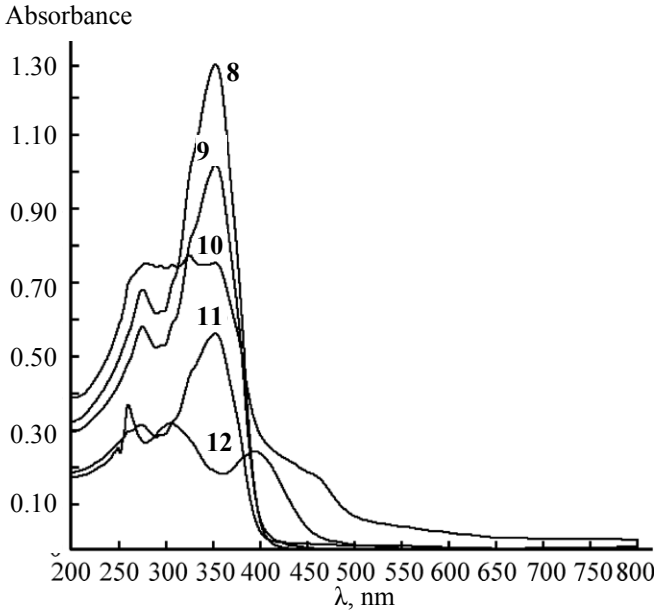

Fig. 3. UV-Vis spectra of complexes **8**–**12** in DMSO.

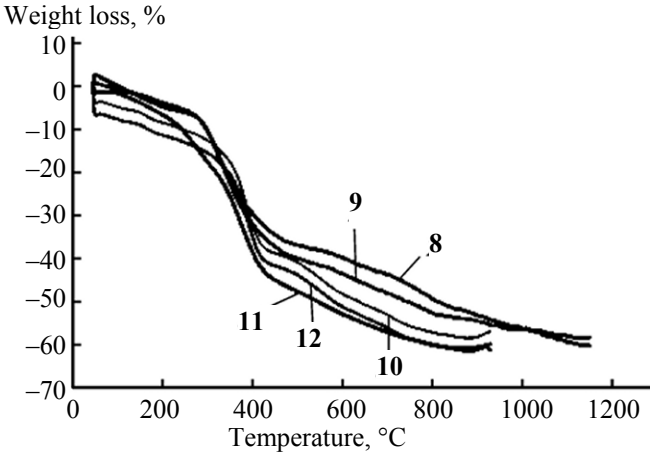

Fig. 4. TG curves of complexes **8**–**12**.

Mn_3O_4. The weight of Mn_3O_4 amounted to 41.5%, which is in a good agreement with the metal analysis.

Iron(II), cobalt(II), and nickel(II) complexes **9**–**11** decomposed in a similar way. Given below are step number, temperature range, lost fragment, weight loss, and incombustible residue: **9**: (1) 46–220°C, $2H_2O$, 5.6%; (2) 225–525°C, $OC_2H_4OC_2H_4OC_2H_4O$, 36.4%; (3) 550–1000°C, $2ArCH{=}NC_6H_4$, 23.0 %; Fe_3O_4 (1100°C); **10**: (1) 46–225°C, $3H_2O$, 9.3%; (2) 230–475°C, $OC_2H_4OC_2H_4OC_2H_4O$, 30.3 %; (3) 500–850°C, $2ArCH{=}NC_6H_4$, 19.2 %; Co_3O_4 (1100°C) [52]; **11**: (1) 46–210°C, $2H_2O$, 6.4%; (2) 225–500°C, $OC_2H_4OC_2H_4OC_2H_4O$, 41.5%; (3) 525–850°C, $2ArCH{=}NC_6H_4$, 13.1%; Ni_2O_3 (1100°C). Thermal decomposition of copper complex **12** included two steps, the first of these resulted in loss of crystallization water (46–220°C, $-2H_2O$, weight loss 5.60%, calcd. 5.62%), and the second step at 225–800°C corresponded to loss of both $OC_2H_4OC_2H_4OC_2H_4O$ and two aniline and aldehyde groups (weight loss 86.00%, calcd. 86.77%); the residue was CuO polluted with some carbon, which remained stable above 800°C.

Antimicrobial and antifungal activity. The antimicrobial activity of the ligands and metal complexes has been screened *in vitro* against the following microorganisms: *Bacillus subtilis* ATCC 6633, *Staphylococcus aureus* ATCC 25923, *Escherichia coli* ATCC 25922, *Enterococcus faecalis* ATCC 29212, *Pseudomonas aeruginosa* ATCC 254992, *Escherichia coli* ATCC 35218, *Bacillus cereus* NRRL B-3711, *Proteus vulgaris* ATCC 13315, *Candida albicans* ATCC 60193, and *Candida tropicalis* ATCC 13803 by the broth micro dilution test [53–56]. The minimal inhibitory concentrations (MICs) of compounds **2**–**7** and complexes **8**–**12** are given in Table 5. The antimicrobial activity spectrum of the examined compounds varied greatly. Compounds **3**–**5** showed a strong antibacterial effect against *Enterococcus faecalis* ATCC 29212. The activity of Fe(II) complex **9** against *Escherichia coli* ATCC 35218 was stronger than that of ampicillin taken as reference. Iron(II), cobalt(II), and copper(II) complexes **9**, **10**, and **12** were more active against *C. albicans* ATCC 60193 than against *C. tropicalis* ATCC 13803. The data in Table 5 indicate that the

Table 5. Antibacterial and antifungal activity (MIC, μg/mL) of compounds **2**–**12**

Microorganism	**2**	**3**	**4**	**5**	**6**	**7**	**8**	**9**	**10**	**11**	**12**	Gentamicin	Ampicillin	Fluconazole
S. aureus	32	32	32	32	32	32	32	16	16	64	32	1	0.016	
E. faecalis	64	16	16	16	64	32	32	16	32	64	64	1	0.016	
B. cereus	64	64	64	64	64	64	32	16	16	64	32	0.125	0.125	
B. subtilis	32	32	32	32	32	64	64	8	16	64	16	0.008	0.06	
E. coli ATCC 25922	128	64	64	128	64	64	64	32	32	64	64	0.125	32	
E. coli ATCC 35218	128	64	64	128	128	64	32	16	16	32	32	0.03	32	
P. aeruginosa	64	64	64	64	64	64	32	16	16	32	32	0.08	2	
P. vulgaris	64	64	64	64	64	64	32	16	16	32	32	0.125	0.06	
C. albicans	32	32	32	32	32	32	32	16	16	32	16			0.0625
C. tropicalis	64	64	64	64	32	32	32	32	32	32	32			0.50

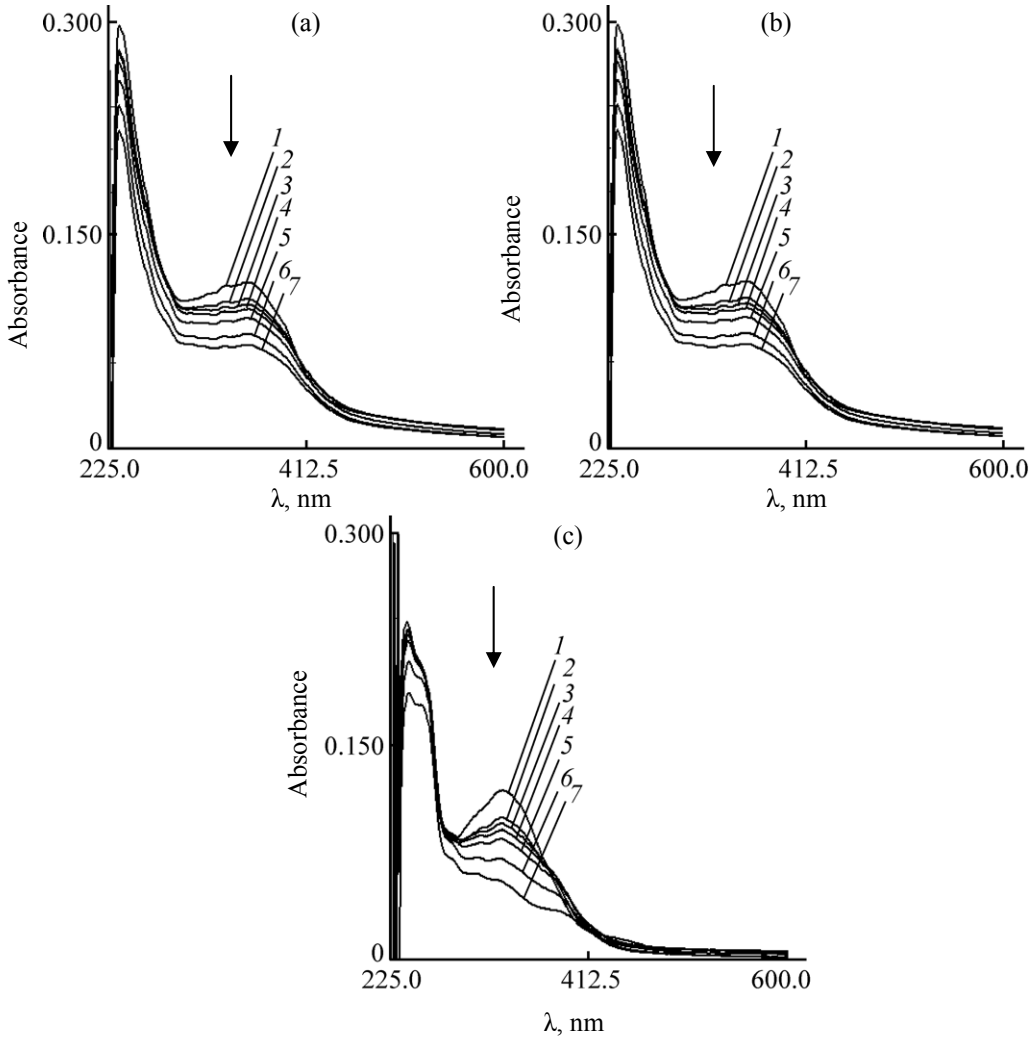

Fig. 5. 5ariation of the electronic absorption spectra of compounds (a) **2**, (b) **4**, and (c) **8** in the presence of increasing amounts of CT-DNA at room temperature in Tris–HCl/NaCl buffer (pH = 7.2); CT-DNA-to-II (**4**, **8**) ratios: 0, 1 : 5, 1 : 2, 1 : 1, 2 : 1, 5 : 1, 10 : 1. DNA concentration: (*1*) 0.0, (*2*) 0.2, (*3*) 0.5, (*4*) 1.0, (*5*) 2.0, (*6*) 5.0, and (*7*) 10.0.

antibacterial activity increases in going from free Schiff base ligand **2** to its metal complexes. This may be explained in terms of the chelation theory [57]. The presence of an azomethine moiety and chelation enhance the antibacterial activity. Among the examined complexes, Fe(II) complex **9** was characterized by the lowest MIC values on the given microorganisms. When a metal ion is chelated by a ligand, its polarity is reduced to a greater extent due to overlap of the ligand orbital and partial sharing of the positive charge of the metal ion with donor groups. In addition, chelation increases delocalization of π electron over the chelate ring, which results in increased lipophilicity of the complex. Consequently, metal complexes more easily penetrate into lipid membranes and block metal binding sites of enzymes of microorganisms. Metal complexes also affect cell respiration and thus block the synthesis of proteins, which restricts further growth of the organism [58]. The new compounds could be selected for further pharmacological tests to be evaluated as potential drugs against many infectious diseases.

DNA binding. DNA binding studies were performed by the spectrophotometric titration technique using Schiff base ligands **2** and **4** and manganese complex **8**. Figure 5 shows variations of the electronic absorption spectra of **2**, **4** and **8** in Tris–HCl/NaCl buffer upon addition of calf thymus (CT) DNA up to a ratio of 10 : 1. The Schiff base ligands and manganese complex in Tris–HCl buffer are characterized by intense π–π* transition bands in the UV region with

Scheme 2. Intercalative binding between DNA and Schiff base podands **2** and **4**.

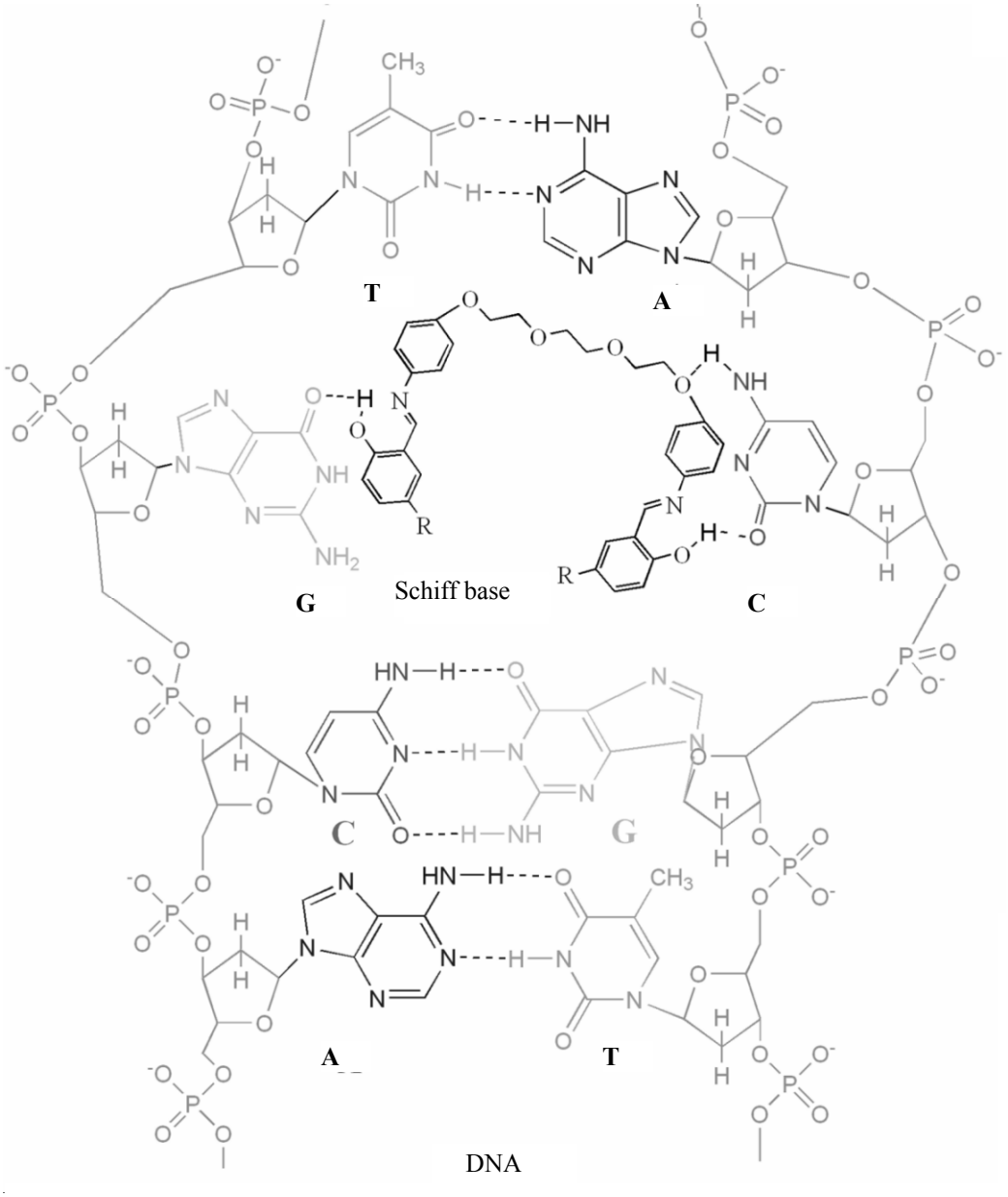

their maxima at 217, 344 (**2**), 234, 358 (**4**), and 239, 329 nm (**8**). As the concentration of CT-DNA increased, the absorption intensity decreased by 5.86–89.45% (**2**), 9.84–37.63% (**4**), and 16.02–40.48% (**8**), and the absorption maxima shift red by 6–11 (**2**), 1–5 (**4**), and 1–3 nm (**8**). According to published data [59–62], hypo(hyper)chromic and batho(hypso)chromic effects in the electronic absorption spectra are related to the degree of intercalative and electrostatic interactions between Schiff bases and CT-DNA. The observed hypochromic effect and bathochromic shift suggest intercalative interaction of Schiff bases **2** and **4** and complex **8** with CT-DNA. Possible mechanisms are shown in Schemes 2 and 3. The Schiff base or complex intercalates between two nucleobases in the DNA molecule. This causes expansion and degradation of DNA molecule.

Anion sensing. The colorimetric response of Schiff base receptors **2**–**7** to various anions in DMSO (5.0×10^{-6} M) was investigated by UV-Vis spectral titration (Fig. 6). The Schiff bases displayed a color change upon addition of fluoride and cyanide ions for **5**, fluoride, cyanide, and hydroxide ions for **6**, and

Scheme 3. Intercalative binding between DNA and Schiff base complex **8**.

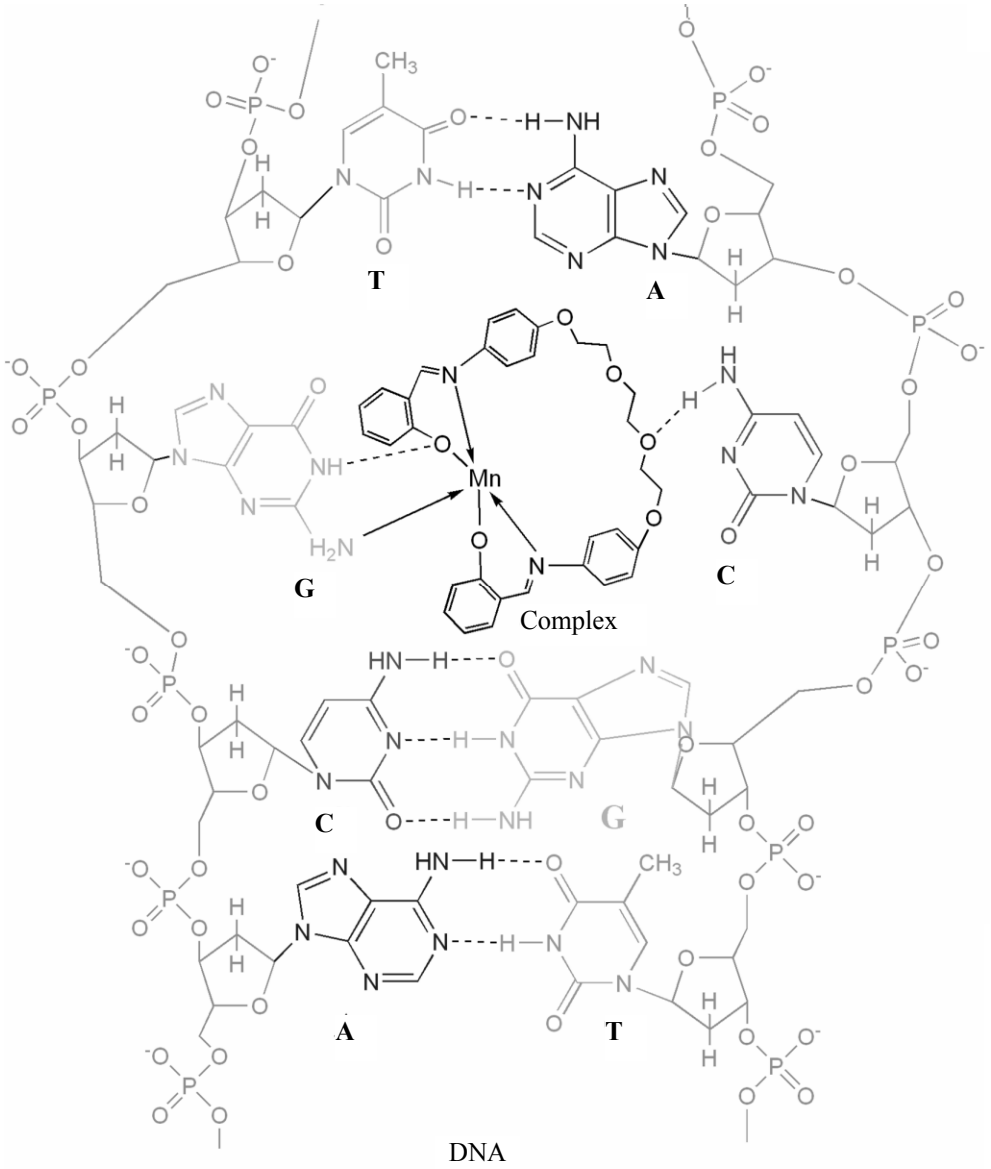

fluoride, cyanide, acetate, and hydroxide ions for **2**–**4** with a substantial bathochromic shift from 342 to 450 nm, but no color change was observed upon addition of bromide, iodide, thiocyanate, perchlorate, dihydrogen phosphate, and hydrogen sulfate ions (Fig. 7). Recently, some publications have identified Schiff bases as potential anion sensors [39–42, 63–66].

Free Schiff base ligand **2**–**6** in DMSO absorb at wavelengths shorter than 400 nm. The presence of OH^-, F^-, CN^- and AcO^- gave rise to absorption bands at $\lambda > 400$ nm (λ_{max} = 435, 437, 450, 422, and 416 nm, respectively). The high selectivity of **2**–**6** for OH^-, F^-, and OAc^- ions may be due to nucleophilicity of these anions in DMSO. The orders of selectivity or affinity for anions are as follows: Schiff base ligand **2**: $F^- > CN^- > OH^- > AcO^-$; **3**: $OH^- > AcO^- > CN^- > F^-$; **4**: $CN^- > OH^- > AcO^- > F^-$; **5**: $CN^- > F^-$; **6**: $OH^- > CN^- > F^- >> H_2PO_4^- \approx Br^- \approx I^- \approx SCN^- \approx ClO_4^- \approx HSO_4^- \approx N_3^-$. The acidic hydroxy group of the enol imine tautomer of **2**–**6** is likely to lose proton on exposure to basic OH^-, F^-, and AcO^- ions, and therefore intramolecular proton transfer to give the ketone amine tautomer is possible [50] (Scheme 4). In contrast, cyanide ion is a much weaker hydrogen acceptor but stronger nucleophile than OH^-, F^-, and AcO^-; so that addition of CN^- to the electron-deficient C=N carbon atom occurs with subsequent fast proton transfer of the

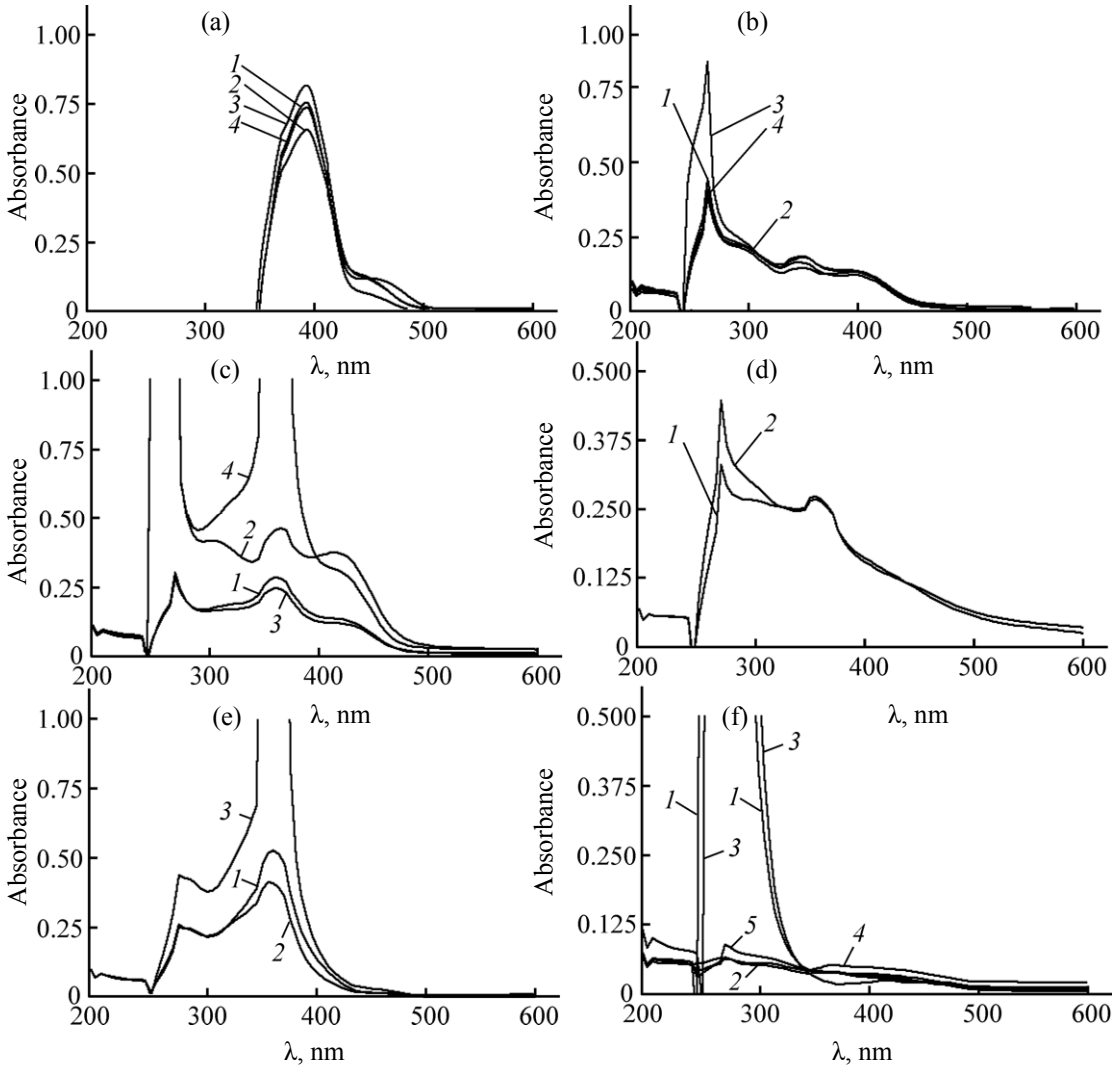

Fig. 6. 5ariation of the electronic absorption spectra of compounds (a) **2**, (b) **3**, (c) **4**, (d) **5**, (e) **6**, and (f) **7** (1 equiv) upon addition of various anions (3 equiv): (*1*) AcO^-, (*2*) CN^-, (*3*) F^-, (*4*) OH^-, (*5*) $H_2PO_4^-$.

phenolic hydrogen atom to the neighboring anionic nitrogen atom through intramolecular hydrogen bond [67] (Scheme 4). The formation of ketone amine tautomer is accompanied by red shift of the absorption maximum. The other anions tested (Br^-, I^-, SCN^-, ClO_4^-, HSO_4^-, $H_2PO_4^-$, N_3^-), being weaker bases than OH^-, F^-, CN^-, and AcO^-, did not induce appreciable shift of the absorption maximum of **2**–**6**.

The interaction of compound **7** with anions is weaker, since it exists in DMSO mainly as the ketone amine tautomer (55%), and proton transfer does not occur in the presence of anions. Thus, the enol form is more efficient as anion sensor. Furthermore, electron-withdrawing substituents in the 5-position increase the sensor properties.

In summary, new Schiff base podands and Mn(II), Fe(II), Co(II), Ni(II), and Cu(II) complexes with one of the former have been synthesized and characterized by elemental analyses, NMR, IR, and UV-Vis spectra, and thermogravimetric data. The Schiff base podands have been found to act as tetradentate chelating ligands through the oxygen and nitrogen atoms of both hydroxy and azomethine groups (metal-to-ligand ratio 1 : 1). Antibacterial and antifungal activities of the ligands and complexes against some bacteria and yeast cultures have also been studied. The metal complexes displayed various inhibitory effects against the bacteria and yeasts. Experimental UV-Vis spectral studies of DNA binding have proved that ligands **2** and **4** and manganese(II) complex **8** can intercalate into CT-DNA, which demonstrates their potential use as DNA

Scheme 4. Probable mechanism of interaction of Schiff bases **2**–**6** with AcO^-, F^-, OH^-, and CN^- ions in DMSO.

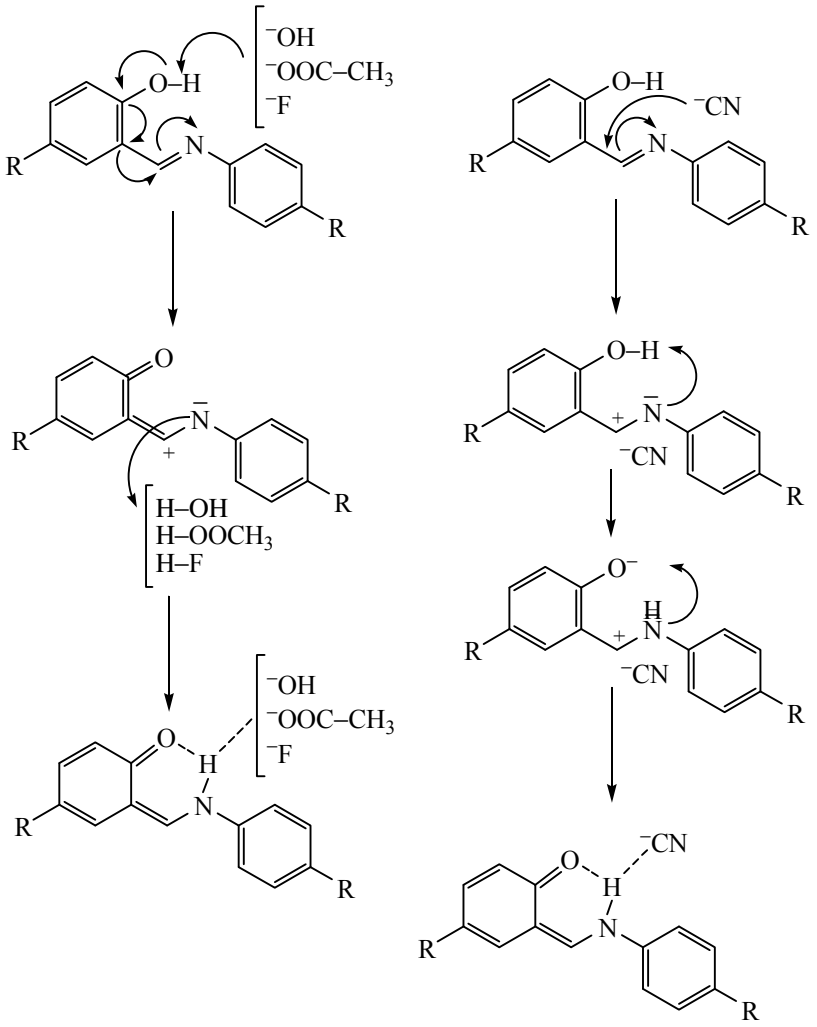

repair agents. Compounds **2**–**6** can act as real-time colorimetric sensors for some anions.

EXPERIMENTAL

The ^1H and ^{13}C NMR spectra were recorded on a Bruker Avance-500 spectrometer operating at 400 and 101.6 MHz, respectively. The infrared absorption spectra were obtained on a Perkin Elmer BX II spectrometer in KBr discs. The UV-Vis spectra were measured using a Shimadzu 1208 Series spectrometer. The elemental analyses were determined on a LECO CHNS-932 analyzer. The melting points were measured on an Electro Thermal IA 9100 apparatus using a capillary tube. 4-Nitrophenol sodium salt, 1,2-bis(2-chloroethoxy)ethane, salicylaldehyde, 5-chlorosalicylaldehyde, 5-bromosalicylaldehyde, 5-hydroxysalicylaldehyde, 5-methoxysalicylaldehyde, 2-hydroxy-1-naphthaldehyde, hydrazine hydrate, Pd/C (10%), MeOH, EtOH, benzene, DMSO, DMF, $MCl_2 \cdot x\,H_2O$ (M = Mn, Fe, Co, Ni, Cu), tetrabutylammonium salts (fluoride, bromide, iodide, cyanide, thiocyanate, perchlorate, hydrogen sulfate, acetate, azide, dihydrogen phosphate, hydroxide), and DNA from calf thymus (CT-DNA: 41.9 mol % G–C and 58.1 mol % A-T. An absorbance of 1.0 at λ = 260 nm corresponds to ~50 μg of double-stranded DNA) were purchased from Sigma–Aldrich (Germany).

Triethylene glycol bis(4-aminophenyl)ether (**1**) was prepared according to the procedure reported in [68].

4,4′-[Ethane-1,2-diylbis(oxyethane-2,1-diyloxy)]-bis[*N*-(2-hydroxybenzylidene)dianiline] (2). Triethylene glycol bis(4-aminophenyl)ether (**1**), 0.50 g (1.50 mmol), was added to a solution of 0.37 g (3.03 mmol) of salicylaldehyde in 100 mL of ethanol. The mixture was refluxed for 2 h under stirring and

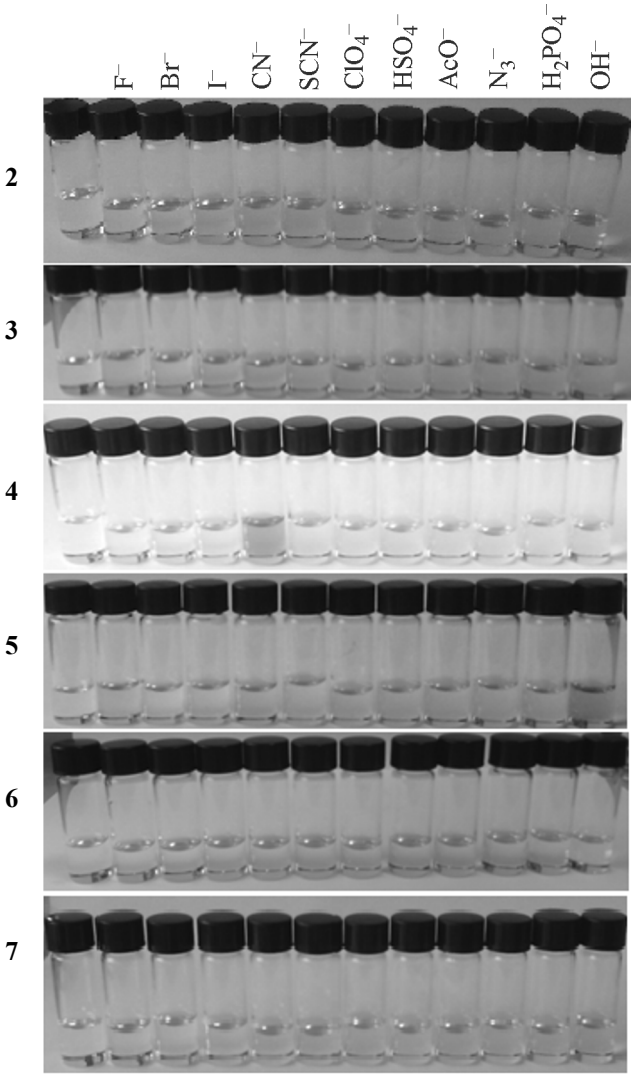

Fig. 7. Color changes of compounds **2**–**7** upon addition of various anions (3 equiv).

evaporated, and the residue was recrystallized from chloroform–*n*-hexane (3 : 1).

Schiff base podands **3**–**7** were synthesized in a similar way. The yields, melting points, and analytical data for compounds **2**–**7** are given in Table 1.

Complexes 8–12 *(general procedure).* A solution of $MnCl_2 \cdot 4\ H_2O$, $FeCl_2 \cdot 4\ H_2O$, $CoCl_2 \cdot 6\ H_2O$, $NiCl_2 \cdot 6\ H_2O$, or $CuCl_2 \cdot 2\ H_2O$ in methanol was added to a solution of compound **2** in the same solvent, the ligand-to-metal molar ratio being 1 : 1. The mixture was heated under reflux for 1 h, and the colored precipitate was filtered off, washed with distilled water, and recrystallized from methanol.

Screening for antimicrobial activity. The minimum inhibitory concentrations (MICs) were evaluated by the broth micro dilution test. A loop full of bacteria was inoculated in 100 mL of nutrient broth in a test-tube shaker at 150 rpm for 20 h at 37°C. Test compounds were dissolved in a minimum volume of DMSO and were serially diluted in a Mueller–Hinton broth to concentrations ranging from 1 to 500 mg/mL (the concentration of compounds in different plates was 500, 250, 125, 62.5, 31.25, 15.6, 8, 4, 2, and 1 μg/mL). The 24-h bacterial cultures were then transferred into 10 mL of Muller-Hinton broth (control and test compounds) and incubated for 24 h at 37°C. The growth of the bacteria was determined by measuring the turbidity after 24 h. The MIC was generally read as the smallest concentration of the drug in the series that prevents the development of visible growth of test organism. The data reported in Table 5 are the average data of three experiments. The data were processed using 13SAS (1990) statistical package program and MINITAB 13.0 statistical analysis software. Differences among the means were tested by the least significant difference (LSD) test at a 5% significance level.

Bacillus subtilis ATCC 6633, *Staphylococcus aureus* ATCC 25923, *Escherichia coli* ATCC 25922, *Enterococcus faecalis* ATCC 29212, *Pseudomonas aeruginosa* ATCC 254992, *Escherichia coli* ATCC 35218, *Bacillus cereus* NRRL B-3711, *Proteus vulgaris* ATCC 13315, *Candida albicans* ATCC 60193, and *Candida tropicalis* ATCC 13803 were used as microorganisms, and gentamicin, ampicillin, and fluconazole were used as controls as they are well known broad-spectrum antibiotics with different mechanisms of activity.

DNA Binding experiments. The UV-Visible spectra titrations were carried out in Tris–HCl/NaCl buffer at room temperature to investigate the binding affinity between CT-DNA and Schiff base Mn(II) complex. Tris–HCl/NaCl buffer (3 mL) and the solutions of Mn(II) complex (3 mL, 1.13×10^{-5} M) were placed into two cuvete s, respectively. Then one aliquot (5 μL, 0.01 M) of buffered CT-DNA solution was added to each cuvettes in order to eliminate the absorbance of DNA itself. Before the absorption spectra were recorded, the compounds-DNA solutions were incubated at room temperature for 5 min.

Anion sensing experiments. Schiff bases (0.05 μmol) were dissolved in DMSO (50 mL). Tetrabutyl-

ammonium salts (F^-, Br^-, I^-, CN^-, SCN^-, ClO_4^-, HSO_4^-, CH_3COO^-, N_3^-, $H_2PO_4^-$, OH^-), 0.05 μmol, were dissolved in DMSO (50 mL). Each tetrabuthylammonium salt solution added to Schiff base solution (1 : 1) in a spectrophotometric cell. After mixing, the electronic absorption spectrum was recorded at room temperature.

ACKNOWLEDGMENTS

The authors thank Çanakkale Onsekiz Mart University Grants Commission for a research grant (Project no. FYL-2013-155).

REFERENCES

1. Mounika, K., Anupama, B., Pragathi, J., and Gyanakumari, C., *J. Sci. Res*. (Rajshahi, Bangladesh), 2010, vol. 2, no. 3, p. 513.
2. Venkatesh, P., *Asian J. Pharm. Health Sci*., 2011, vol. 1, p. 8.
3. Yıldız, M., Dülger, B., Koyuncu, S.Y., and Yapıcı, B.M., *J. Indian Chem. Soc*., 2004, vol. 81, p. 7.
4. Ünver, H., Yıldız, M., Dülger, B., Özgen, Ö., Kendi, E., and Durlu, T.N., *J. Mol. Struct*., 2005, vol. 737, p. 159.
5. Yıldız, M., Ünver, H., Dülger, B., Erdener, D., Ocak, N., Erdönmez, A., and Durlu, T.N., *J. Mol. Struct*., 2005, vol. 738, p. 253.
6. Yıldız, M., Dülger, B., and Çınar, A., *J. Indian Chem. Soc*., 2005, vol. 82, p. 414.
7. Yıldız, M., Kiraz, A., and Dülger, B., *J. Serb. Chem. Soc*., 2007, vol. 72, no. 3, p. 215.
8. Kiraz, A., Yıldız, M., and Dülger, B., *Asian J. Chem*., 2009, vol. 21, no. 6. p. 4495.
9. Sondhi, M., Singh, N., Kumar, A., Lozach, O., and Meijer, L., *Bioorg. Med. Chem*., 2006, vol. 14, no. 11, p. 3758.
10. Budakoti, A., Abid, M.M., and Azam, A., *Eur. J. Med. Chem*., 2006, vol. 41, p. 63.
11. Pandey, A., Dewangan, D., Verma, S., Mishra, A., and Dubey, R.D., *Int. J. Chem. Tech. Res*., 2011, vol. 3, p. 178.
12. Chandramouli, C., Shivanand, M.R., Nayanbhai, T.B., Bheemachari, B., and Udupi, R.H., *J. Chem. Pharm. Res*., 2012, vol. 4, no. 2, p. 1151.
13. Chinnasamy, R.P., Sundararajan, R., and Govindaraj, S., *J. Adv. Pharm. Technol. Res*., 2010, vol. 1, no. 3, p. 342.
14. Chaubey, A.K. and Pandeya, S.N., *Int. J. Pharm. Tech. Res*., 2012, vol. 4, no. 4, p. 590.
15. Aboul-Fadl, T., Mohammed, F.A., and Hassan, E.A., *Arch. Pharm. Res*., 2003, vol. 26, no. 10, p. 778.
16. Miri, R., Razzaghi-asl, N., and Mohammadi, M.K., *J. Mol. Model*., 2013, vol. 19, no. 2, p. 727.
17. Ali, S.M.M., Azad, M.A.K., Jesmin, M., Ahsan, S., Rahman, M.M., Khanam, J.A., Islam, M.N., and Shahriar, S.M.S., *Asian Pac. J. Trop. Biomed*., 2012, vol. 2, no. 6, p. 438.
18. Wei, D., Li, N., Lu, G., Yao, K., *Sci. China, Ser. B: Chem*., 2006, vol. 49, no. 3, p. 225.
19. Avaji, P.G., V inod Kumar, C.H., Patil, S.A., Shivananda, K.N., and Nagaraju, C., *Eur. J. Med. Chem*., 2009, vol. 44, no. 9, p. 3552.
20. Cozzi, P.G., *Chem. Soc. Rev*., 2004, vol. 33, p. 410.
21. Chandra, S. and Sangeetika, J., *J. Indian Chem. Soc*., 2004, vol. 81, p. 203.
22. Chohan, Z.H., Praveen, M., and Ghaffar, A., *Met.-Based Drugs*, 1997, vol. 4, no. 5, p. 267.
23. Suslick, K.S., and Reinert, T.J., *J. Chem. Educ*., 1988, vol. 62, p. 974.
24. Bottcher, A., Takeuchi, T., Simon, M.I., Meade, T.J., and Gray, H.B., *J. Inorg. Biochem*., 1995, vol. 59, p. 221.
25. Qiao, X., Ma, Z.-Y., Xie, C.-Z., Xue, F., Zhang, Y.-W., Xu, J.-Y., Qiang, Z.-Y., Lou, J.-S., Chen, G.-J., and Yan, S.-P., *J. Inorg. Biochem*., 2011, vol. 105, p. 728.
26. Chaviara, A.T., Cox, P.J., Repana, K.H., Papi, R.M., Papazisis, K.T., Zambouli, D., Kortsaris, A.H., Kyriakidis, D.A., and Bolos, C.A., *J. Inorg. Biochem*., 2004, vol. 98, p. 1271.
27. Chaviara, A.T., Cox, P.J., Repana, K.H., Pantazaki, A.A., Papazisis, K.T., Kortsaris, A.H., Kyriakidis, D.A., Nikolov, G.S., and Bolos, C.A., *J. Inorg. Biochem*., 2005, vol. 99, p. 467.
28. Xie, C.-Z., Sun, M.-M. M.-M., Li, S.-H., Zhang, X.-T., Qiao, X., Ouyang, Y., and Xu, J.-Y., *J. Coord. Chem*., 2013, vol. 66, no. 22, p. 3891.
29. Qiao, X., Ma, Z.-Y., Shao, J., Bao, W.-G., Xu, J.-Y., Qiang, Z.-Y., and Lou, J.-S., *BioMetals*, 2014, vol. 27, no. 1, p. 155.
30. Roy, S., Maheswari, P.U., Lutz, M., Spek, A.L., Dulk, H., Barends, S., van Wezel, G.P., Hartl, F., and Reedijk, J., *Dalton Trans*., 2009, p. 10 846.
31. de Hoog, P., Louwerse, M.J., Gamez, P., Pitié, M., Baerends, E.J., Meunier, B., and Reedijk, J., *Eur. J. Inorg. Chem*., 2008, p. 612.
32. Pachon, L.D., Golobic, A., Kozlevcar, B., Gamez, P., Kooijman, H., Spek, A.L., and Reedijk, J., *Inorg. Chem. Acta*, 2004, vol. 357, p. 3697.
33. Maheswari, P.U., Barends, S., Yaman, S.O., de Hoog, P., Casellas, H., Teat, S.J., Massera, C., Lutz, M., Spek, A.L., van Wezel, G.P., Kozlevcar, B., Gamez, P., and Reedijk, J., *J. Am. Chem. Soc*., 2006, vol. 128, p. 710.
34. Dalapati, S., Alam, M.A., Jana, S., and Guchhait, N., *J. Fluorine Chem*., 2011, vol. 132, p. 536.
35. Samanta, A., Dalapati, S., and Guchhait, N., *J. Photochem. Photobiol., A*, 2012, vol. 232, p. 64.

36. Moragues, M.E., Martínez-Máñez, R., and Sancenón, F., *Chem. Soc. Rev*., 2011, vol. 40, p. 2593.
37. Gale, P.A., García-Garrido, S.E., and Garric, J., *Chem. Soc. Rev*., 2008, vol. 37, p. 151.
38. Steed, J.W., *Chem. Soc. Rev*., 2009, vol. 38, p. 506.
39. Dalapati, S., Alam, M.A., Jana, S., Karmakar, S., and Guchhait, N., *Spectrochim. Acta, Part A*, 2013, vol. 102, p. 314.
40. Dalapati, S., Alam, M.A., Jana, S., and Guchhait, N., *Sens. Actuators, B*, 2012, vol. 162, p. 57.
41. Dalapati, S., Jana, S., and Guchhait, N., *Chem. Lett*. 2011, vol. 40, p. 279.
42. Dalapati, S., Jana, S., Alam, M.A., and Guchhait, N., *Sens. Actuators, B*, 2011, vol. 160, p. 1106.
43. Yıldız, M., Kılıç, Z., and Hökelek, T., *J. Mol. Struct*., 1998, vol. 441, p. 1.
44. Nazır, H., Yıldız, M., Yılmaz, H., Tahir, M.N., and Ülkü, D., *J. Mol. Struct*., 2000, vol. 524, p. 241.
45. Yıldız, M., Unver, H., Erdener, D., Kiraz, A., and İskeleli, N.O., *J. Mol. Struct*., 2009, vol. 919, p. 227.
46. Ünver, H. and Yıldız, M., *Spectrosc. Lett*., 2010, vol. 43, p. 114.
47. Ünver, H., Yıldız, M., Özay, H., and Durlu, T.N., *Spectrochim. Acta. Part A*, 2009, vol. 74, p. 1095.
48. Özay, H., Yıldız, M., Ünver, H., and İskeleli, N.O., *Synth. React. Inorg., Met.-Org. Nano-Met. Chem*., 2012, vol. 42, no. 6, p. 872.
49. Hökelek, T., Akduran, N., Yıldız, M., and Kılıç, Z., *Anal. Sci*., 2000, vol. 16, p. 553.
50. Yıldız, M., *Spectosc. Lett*., 2004, vol. 37, no. 4, p. 367.
51. Yeap, G.-Y., Ha, S.-T., Ishizawa, N., Suda, K., Boey, P.-L., and Mahmood, W.A.K., *J. Mol. Struct*., 2003, vol. 658, p. 87.
52. Devi, G.I., Sabu, P.G., and Geetha, P., *Res. J. Chem. Sci*., 2013, vol. 3, no. 9, p. 58.
53. Amsterdam, D., *Antibiotics in Laboratory Medicine*, Lorian, V., Ed., Baltimore: Williams & Wilkins, 1996, 4th ed., p. 111.
54. Wiegand, I., Hilpert, K., and Hancock. R.E.W., *Nat. Protoc*., 2008, vol. 3, no. 2, p. 163.
55. Rodríguez-Tudela, J.L., Barchiesi, F., Bille, J., Chryssanthou, E., Cuenca-Estrella, M., Denning, D., Donnelly, J.P., Dupont, B., Fegeler, W., Moore, C., Richardson, M., and Verweij, P.E., *Clin. Microbiol. Infect*., 2003, vol. 9, no. 8, p. i.
56. Miller, R.A., Walker, R.D., Carson, J., Coles, M., Coyne, R., Dalsgaard, I., Gieseker, C., Hsu, H.M., Mathers, J.J., Papapetropoulou, M., Petty, B., Teitzel, C., and Reimschuessel, R., *Dis. Aquat. Org*., 2005, vol. 64, no. 3, p. 211.
57. Mishra, L. and Singh, V.K., *Indian J. Chem., Sect. A*,, 1997, vol. 32, p. 446.
58. Padmaja, M., Pragathi, J., Anupama, B., and Kumari, C.G., *J. Chem*., 2012, vol. 9, no. 4, p. 2145.
59. Arjmand, F. and Aziz, M., *Eur. J. Med. Chem*., 2009, vol. 44, no. 2, p. 834.
60. Qiao, X., Ma, Z.-Y., Xie, C.-Z., Xue, F., Zhang, Y.-W., Xu, J.-Y., Qiang, Z.-Y., Lou, J.-S., Chen, G.-J., and Yan, S.-P., *J. Inorg. Biochem*., 2011, vol. 105, p. 728.
61. Dehghan, G., Dolatabadi, J.E.N., Jouyban, A., Zeynali, K.A., Ahmadi, S.M., and Kashanian, S., *DNA Cell Biol*., 2011, vol. 30, p. 195.
62. Hiort, C., Lincoln, P., and Norden, B., *J. Am. Chem. Soc*., 1993, vol. 115, p. 3448.
63. Sharma, D., Mistry, A.R., Bera, R.K., and Sahoo, S.K., *Supramol. Chem*., 2013, vol. 25, no. 4, p. 212.
64. Ge, L. and Jie, S., *J. Inclusion Phenom. Macrocyclic Chem*., 2013, vol. 76, p. 99.
65. Sasanka, D., Sankar, J., and Nikhil, G., *Spectrochim. Acta, Part A*, 2014, vol. 129, p. 499.
66. Samit, G and Sourav, S., *J. Am. Chem. Soc*., 2010, vol. 132, p. 17 674.
67. Noh, J.Y., Hwang, I.H., Kim, H., Song, E.J., Kim, K.B., and Kim, C., *Bull. Korean Chem. Soc*., 2013, vol. 34, no. 7, p. 1985.
68. Dutasta, J.P., Declercq, J.P., Calderon, C.E., and Tinant, B., *J. Am. Chem. Soc*., 1989, vol. 111, p. 7136.